

# Nonlinear quantum search via coined quantum walks

Basile Herzog\*

*Aix-Marseille Université, CNRS, LIS, Marseille, France and  
Université de Lorraine, LPCT, Nancy, France*

Giuseppe Di Molfetta<sup>†</sup>

*Aix-Marseille Université, CNRS, LIS, Marseille, France*

(Dated: September 17, 2020)

We provide first evidence that some families of nonlinear quantum systems, rephrased in terms of coined quantum walks with effective nonlinear phase, display a strong computational advantage for search algorithms, over graphs having sets of vertices of constant size, e.g. the infinite square grid. The numerical simulations show that the walker finds the marked vertex in  $O(N^{1/4} \log^{3/4} N)$  steps with probability  $O(1/\log N)$ , for an overall complexity of  $O(N^{1/4} \log^{7/4} N)$ . We also confirm this result analytically. Moreover the algorithm is implemented without the need for a specific oracle step, but by topological hole defect in the grid. From a quantum computing perspective, however, this hints at novel applications of quantum walk search: instead of using them to look for "good" solutions within the configuration space of a problem, we could use them to look for topological properties of the entire configuration space.

## I. INTRODUCTION

Searching an element among an unstructured database of size  $N$  takes  $O(N)$  iterations, resulting in a linear complexity time. In 1996, L. Grover came up with a quantum algorithm it speeds up any brute force  $O(N)$  problem into a  $O(\sqrt{N})$  problem [12]. The algorithm comes in many variants and has been rephrased in many ways, including in terms of quantum walks [8]. Quantum walks (QW) are essentially local unitary gates that drive the evolution of a particle on a graph [21], and although they may appear defined in a discrete and in a continuous time setting, recently it has been shown that a new family of "plastic" QW unify and encompass both systems [9, 16]. They have been used as a mathematical framework to express many quantum algorithms e.g. [3, 5, 6], but also many quantum simulation schemes e.g. [11, 13]. In particular, it has been shown that many of these QW admit, as their continuum limit, the Dirac equation [4, 10], providing 'quantum simulation schemes', for the future quantum computers, to simulate all free spin-1/2 fermions. More interestingly, it has been recently proven by one of the authors, that the Grover algorithm is indeed a naturally occurring phenomenon, i.e. spontaneously implemented by some kind of particles in nature [19] over arbitrary surfaces with topological defects. From a theoretical perspective, a Grover search on a graph, rephrased in terms of QW, is an alternation of the diffusion step and the oracle. The nodes of the graph, represent elements of the configuration space of a problem, and whose edges represent the existence of a local transformation between two configurations. So far, the QW search has only been

used to look for 'marked nodes', i.e. good configurations within the configuration space, as specified by an oracle. In [19], it has been proved that instead of using them to look for 'good' solutions within the configuration space of a problem, we could use them to look for topological properties of the entire configuration space. Here we will position ourselves in the same theoretical groove, but in a nonlinear framework.

The generalisation to an interacting multi-walkers scenario has never been explored in quantum algorithms, although one unpublished result has shown that a nonlinear effective potential, embedded in the QW evolution operator may improve the searching time [14]. Moreover, considering nonlinear effective terms to investigate the multi-particle case, makes the simulation feasible classically. Indeed, there exists many physical systems which may be described by a nonlinear effective equation, such as the Bose-Einstein condensates, making these models physically implementable [2, 15]. From a more theoretical point of view, the growing interest for such systems started with Abrams and Lloyd, showing that nonlinearity in quantum computation, could make quantum systems solve NP-complete problems in polynomial time [1].

In particular, nonlinearity in Quantum Walks have been considered in several recent studies and may appear or under the form of nonlinear phases, (e.g. in Kerr medium [17] and [18]) either via a feed-forward quantum diffusion operator [20]. In this manuscript we will give numerical and analytical evidence that nonlinearity leads to a clear computational advantage on the two dimensional grid respect to the linear case, consistently with previous results on the hypercube [22], paving the way to extend our nonlinear scheme in higher dimensional physical dimensions.

---

\*Electronic address: basile.herzog@gmail.com

<sup>†</sup>Electronic address: giuseppe.dimolfetta@lis-lab.fr

The manuscript is organized as follows : In Section II, we will introduce the QW in continuous time and dis-

crete space; in Section III we will presents our numerical simulations for the linear and nonlinear algorithm and in Section IV we will derive analytically the probability peak recurrence time. Finally, in Section V, we discuss the results and conclude.

## II. MODEL

### A. The linear algorithm

Quantum Walks in continuous time are defined on a  $N$ -vertices non directed graph  $G \equiv G(V, E)$  with  $V$  a set of vertices, where the corresponding Hilbert space is  $\mathcal{H} = \text{span}\{|v\rangle : v \in V\}$ , and  $E$  a set of edges linking two vertices :  $E \subseteq \{(x, y) | (x, y) \in V^2\}$ . A state  $|\psi(t)\rangle$ ,  $t \in \mathbb{R}^+$  being the time parameter, is generally written in the basis  $|v\rangle$ ,  $|\psi(t)\rangle = \sum_{v \in V} p_v(t) |v\rangle$ , where the complex amplitudes  $p_v(t) = \langle v | \psi(t) \rangle$ .

The evolution of  $|\psi(t)\rangle$  obeys to the Schrödinger equation:

$$i \frac{dp_v(t)}{dt} = \sum_w H_{vw} p_w(t) \quad (1)$$

where  $H_{vw}$  are the coefficients of the Hamiltonian  $H$ , governing the dynamics. The above evolution is formally close to a classical continuous time Markov process, in imaginary time, where the Hamiltonian plays the role of a discrete Laplacian.

In this framework, the search problem corresponds to find a vertex  $|\bar{v}\rangle$ , given a state vector  $|\psi(t=0)\rangle$  initialized as the uniform superposition over each vertex :

$$|\psi(0)\rangle = \frac{1}{\sqrt{N}} \sum_{v \in V} |v\rangle. \quad (2)$$

Although the above equation works for any arbitrary graph, in the following, we will choose a 2D-square lattice of  $N = L^2$  vertices, labeled by  $\mathbf{v} = (v_1, v_2) \in [L]^2$ , with  $[L] = \{0, 1, \dots, L-1\}$ , evolving in the Hilbert space

$$\mathcal{H} := \text{span}\{|v\rangle : v \in [L]^2\} \quad (3)$$

where the vector  $(v_1, v_2)$  accounts the internal states of the walker, namely the coin states, as in [7]. The Hamiltonian reads :

$$H_0 |v\rangle = (-1)^{v_1} (|v + \mathbf{e}_1\rangle - |v - \mathbf{e}_1\rangle) \quad (4)$$

$$+ (-1)^{v_1+v_2} (|v + \mathbf{e}_2\rangle - |v - \mathbf{e}_2\rangle) \quad (5)$$

$\mathbf{e}_1$  and  $\mathbf{e}_2$  being the basis of the lattice with coordinates  $(1, 0)$  and  $(0, 1)$ .

The 2D-grid is factorised into crystals of  $n = N/4$  cells. Each cell is a square composed of four vertices (items). The new coordinates system is defined by  $\mathbf{x}$ , labelling the cell, such that  $\mathbf{x} \in [l]^2$  with  $l = L/2$ , and by  $\boldsymbol{\sigma} \in \mathbb{Z}_2^2$ , labelling the item inside each cell. In particular, we

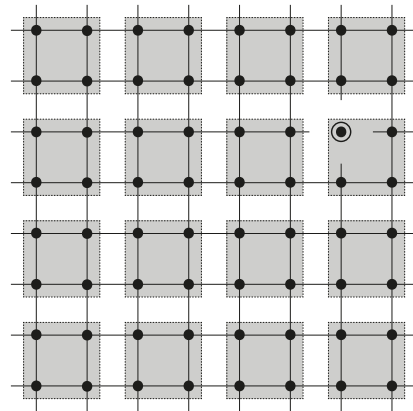


FIG. 1: The  $2d$ -grid and its factorisation into cells (grey squares). The marked vertex (circled) is disconnected from its neighbors.

can write the following transformations, which map the vertices into cell coordinates :

$$x_i = \left\lfloor \frac{v_i}{2} \right\rfloor \quad (6)$$

$$\sigma_i = v_i - 2x_i \quad (7)$$

$\lfloor \cdot \rfloor$  denoting the floor function.

Then the searched vertex is :

$$|\bar{v}\rangle = |\mathbf{w}, \boldsymbol{\alpha}\rangle \quad (8)$$

with  $\mathbf{w} \in [l]^2$  and  $\boldsymbol{\alpha} \in \mathbb{Z}_2^2$  and, the oracle Hamiltonian is defined by :

$$H_{oracle} = -|\mathbf{w}, \boldsymbol{\alpha}\rangle \langle \mathbf{w}, \boldsymbol{\alpha}| H_0 - H_0 |\mathbf{w}, \boldsymbol{\alpha}\rangle \langle \mathbf{w}, \boldsymbol{\alpha}|. \quad (9)$$

Notice that the above Hamiltonian,  $H_{oracle}$ , added to  $H_0$ , has the effect of disconnecting the marked vertex from his neighborhood, as in Fig. 1. Indeed, by the definition,  $\langle v | H_0 |v\rangle = \langle \mathbf{w}, \boldsymbol{\alpha} | H_0 | \mathbf{w}, \boldsymbol{\alpha}\rangle = 0$ , and it follows that  $H_L | \mathbf{w}, \boldsymbol{\alpha}\rangle = (H_{oracle} + H_0) | \mathbf{w}, \boldsymbol{\alpha}\rangle = -| \mathbf{w}, \boldsymbol{\alpha}\rangle \langle \mathbf{w}, \boldsymbol{\alpha} | H_0 | \mathbf{w}, \boldsymbol{\alpha}\rangle - H_0 | \mathbf{w}, \boldsymbol{\alpha}\rangle + H_0 | \mathbf{w}, \boldsymbol{\alpha}\rangle = 0$ . As consequence, one can not reach the neighbors of  $| \mathbf{w}, \boldsymbol{\alpha}\rangle$  from itself. Moreover, one can not reach  $| \mathbf{w}, \boldsymbol{\alpha}\rangle$  from its neighbors neither, because the total Hamiltonian  $H_L$  is real and then it has to be symmetric.

More interestingly, one could remark that the isolated vertex introduces a topological defect in the grid, because the disconnected links reduce the connectivity of the neighborhood. Then, one may argue that any natural system described by  $H_L$ , diffusing on a surface with a topological hole defect, can naturally implement a Grover search, as it has been recently proven by one of the authors, in the discrete-time setting [19].

In conclusion, searching the marked vertex  $|\bar{v}\rangle$  formally coincides to search the state (10):

$$|\Gamma\rangle = \frac{1}{2} H_0 | \mathbf{w}, \boldsymbol{\alpha}\rangle. \quad (10)$$

or more formally, by implementing the following algorithm:

---

**Algorithm 1:** Searching algorithm for the  $2d$ -grid

---

Initialization :

$$|\psi\rangle = |s\rangle;$$

$$t = 0;$$

**while**  $t < T = O(\sqrt{N \log N})$  **do**

$$|\psi\rangle = H_L |\psi\rangle;$$

$$t = t + 1;$$

**end**

Measure  $|\psi\rangle$

---

where the initial state reads:

$$|s\rangle = \sqrt{\frac{4}{N}} \sum_{\mathbf{x} \in [l]^2} |\mathbf{x}, \alpha\rangle \quad (11)$$

In order to justify  $T$ , let us recall that, in the linear case, the system evolves approximately between the states  $\frac{1}{\sqrt{2}}(|\Psi_- \rangle - |\Psi_+ \rangle) \approx |s\rangle$  and  $\frac{1}{\sqrt{2}}(|\Psi_- \rangle + |\Psi_+ \rangle) \approx |\Gamma\rangle$ , where the states  $|\Psi_{\pm}\rangle$  are two eigenvectors of the Hamiltonian  $H_L$ , with respective eigenvalues

$$E_{\pm} \approx \pm \sqrt{\frac{64\pi}{N \log N}}. \quad (12)$$

And notice that, in this basis, the Hamiltonian reads:

$$H_L = \begin{pmatrix} 0 & E \\ E & 0 \end{pmatrix} \quad (13)$$

with eigenvalues  $E_{\pm} = \pm E$ . Then, the probability to be projected on the state  $|\Gamma\rangle$  is

$$|\langle \Gamma | \psi(t) \rangle|^2 \approx \frac{\pi}{\log N} \sin^2(Et) \quad (14)$$

which means that, the system will be sufficiently close to the state  $|\Gamma\rangle$ , in a time  $T = \pi/E = O(\sqrt{N \log N})$ .

### B. Adding a nonlinearity

Now, let us consider a walker, driven by a nonlinear Hamiltonian. Among all possible choices, we decided to consider the most common, *i.e.*, a nonlinear diagonal potential, which, physically speaking, corresponds to a Kerr nonlinearity. More formally, we add to the total Hamiltonian  $H_L$ , the following operator:

$$H_{NL} = g \sum_{i=1}^N |\langle i | \psi(t) \rangle|^2 |i\rangle\langle i| \quad (15)$$

where  $g$  is a coupling real coefficient. The new Hamiltonian  $H_L + H_{NL}$  is now time-dependent and in general it is not spanned by the basis  $\{|s\rangle, |\Gamma\rangle\}$ . However, we

can rescale the linear part of the Hamiltonian in such a way, the system, under certain conditions, still evolves between those two states.

First, let's define  $a(t)$  and  $b(t)$  at time  $t$  as follows :

$$|a|^2 = |\langle \Gamma | \Psi(t) \rangle|^2 \quad (16)$$

$$|b|^2 = |\langle s | \Psi(t) \rangle|^2. \quad (17)$$

The two-states system now reads:

$$\begin{pmatrix} \frac{g|a|^2}{4} & E \\ E & \frac{4g|b|^2}{N} \end{pmatrix}. \quad (18)$$

By subtracting  $\frac{4g|b|^2}{N}$  to the diagonal coefficients, the dynamics keeps unchanged and we get:

$$\begin{pmatrix} g\delta & E \\ E & 0 \end{pmatrix} \quad (19)$$

with

$$\delta(t) = \left( \frac{|a|^2}{4} - \frac{4|b|^2}{N} \right). \quad (20)$$

The new eigenvalues are now:

$$\lambda_{\pm} = \frac{1}{2}g\delta \pm \frac{1}{2}\sqrt{(g\delta)^2 + 4E^2} \quad (21)$$

with eigenvectors, respectively:

$$|\phi_{\pm}\rangle = \left( \frac{g\delta}{2E} \pm \frac{\sqrt{(g\delta)^2 + 4E^2}}{2E}, 1 \right). \quad (22)$$

Let us recall that, in several systems, it is possible to rescale the linear part of the global Hamiltonian by multiplying the linear part,  $H_L$ , by a factor depending on the terms  $|a|^2$ ,  $|b|^2$  and  $N$ , to force the system to oscillate between  $s$  and  $\Gamma$ . As an example, in the hypercube graph, it is possible to factorize the main term  $|a|^2$  of the nonlinearity in the oracle, as detailed in [22]. However, here, in  $H_L$ , the diffusion term,  $H_0$ , needs to have the same weight as the oracle, to ensure the disconnection of the marked vertex, which means that we cannot tune  $H_0$  independently. At the same time, the oracle is not globally proportional to the projector  $|\Gamma\rangle\langle\Gamma|$ , as in the hypercube case, so we cannot factorize  $|a|^2$  in the same way.

The solution we propose here, is to change  $E$ , keeping the perturbation  $g\delta$  sufficiently small. By multiplying the Hamiltonian  $H_L$  by a term  $(1 + c(N)g\delta)$ , with  $c(N)$  a real function of  $N$ , the initial eigenvalue  $E$  transforms as :

$$E \rightarrow E' = E(1 + c(N)g\delta). \quad (23)$$

Now, in order to rescale the eigenvectors of the equation 22 as in the form  $(\pm 1, 1)$ , we need to impose  $2E(1 + c(N)g\delta) \gg g\delta$ , which implies that :

$$c(N) \gg \frac{1}{2E} - \frac{1}{g\delta}. \quad (24)$$

Also, the term  $1 + cg\delta$  must be different from zero, otherwise we would not have any diffusion of the walker. For  $t = 0$ , we have  $\delta(0) = -\frac{4|b|^2(0)}{N}$ , and  $|b|^2(t=0) = 1$  as  $|\psi(t=0)\rangle = |s\rangle$ . This yields an upper bound on  $c(N)$  :

$$c(N) < c_{max} = \frac{N}{4g}. \quad (25)$$

Now, keeping only the leading term  $1/2E$  in the lower bound for  $c$ , we end up with

$$\frac{N}{4g} > c \gg \frac{1}{2} \sqrt{\frac{N \log N}{64\pi}} = \frac{1}{2E}. \quad (26)$$

In particular, the above inequality also implies that  $g$  can not scale faster than  $\sqrt{N}$ .

Finally, we replace in the algorithm 1 the linear Hamiltonian by the rescaled one, we add the nonlinear part and we get :

---

**Algorithm 2:** Searching with a nonlinear algorithm for the  $2d$ -grid

---

Initialization :

$$|\psi\rangle = |s\rangle;$$

$$t = 0;$$

**while**  $t < T'$  **do**

$$|\psi\rangle = ((1 + gc\delta) H_L + H_{NL}) |\psi\rangle;$$

$$t = t + 1;$$

**end**

Measure  $|\psi\rangle$

---

Contrary to the linear algorithm 1, an exact analytical treatment to explicitly calculate  $T'$  is not possible. In the following, first, we will provide strong numerical evidence that such a search scheme allows a clear temporal advantage over the linear case, deriving numerically  $T'$  and second, we will give an approximate analytical proof for it.

### III. NUMERICAL RESULTS

Numerical simulations show in Fig. 2 the first peak probability time  $T'$  in function of  $c$  at fixed  $N$  and the corresponding probability peaks for several values of  $c$ , in Fig. 3. In all cases, we have chosen  $g = \log N/\pi$ , which ensures that  $g\delta \sim 1$ . Notice that, for  $c = 0$  the running time  $T'$  is the same as the linear algorithm,  $T$ , but the first probability peak is lower, as the initial eigenstate  $|s\rangle$  doesn't rotate to the state  $|\Gamma\rangle$ , as well as in the linear case. In Fig 2, we can also remark that the probability peak becomes narrower, the more  $c$  increases, which would require more attempts to estimate the maximum of the probability curve, making the algorithm sub-optimal

[22]. These considerations suggest to choose a value for  $c$  which, while ensuring good oscillatory behaviour of the system, leaves the peaks wide enough. A good enough example is  $c = 1/E = \sqrt{\frac{N \log N}{64\pi}} \approx 5.52$ , as one can see in Fig. 3. Let us keep this value for  $c$  in the following for the data analysis.

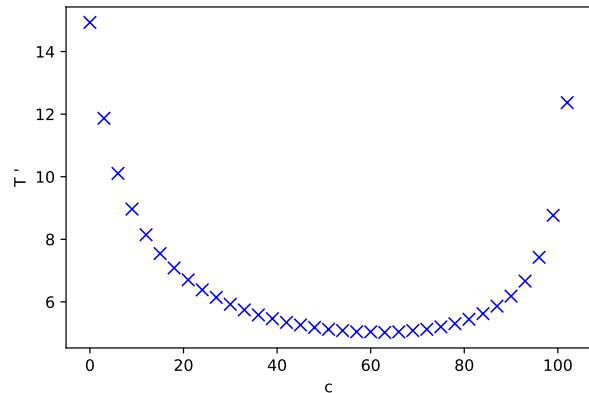


FIG. 2: Run time of the algorithm as a function of  $c$ ,  $N = 900$ .

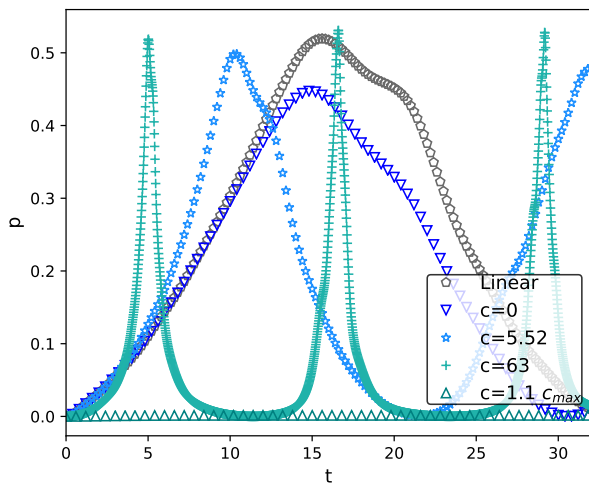


FIG. 3: Probability over  $|\Gamma\rangle$  for different values of  $c$  -  $N = 900$

Now, we proceed as follows : (i) Prepare, the initial state as in (11) ; (ii) Let the walker evolve with time; (iii) Quantify the number of steps  $T(N), T'(N)$  before the walker reaches its probability peak  $\bar{p}(N)$  of being localized in a ball of radius 1 around the center of the defect, namely the peak recurrence time, respectively for the linear and nonlinear search algorithm. Then, estimate this probability peak, at fixed  $N$  ; (iv) Characterize  $T(N), T'(N)$  and  $\bar{p}(N)$ , i.e. the way the peak recurrence times and the probability peak depend upon the total

number grid points. We run both algorithm, the linear and the nonlinear one and we derive from both, a numerical characterization for  $T(N)$ ,  $T'(N)$  and  $\bar{p}(N)$ . The peak probability in the linear and in the nonlinear case, behaves as  $1/\log(N)$ , as it is shown in Fig. 4, approximately with the same pre-factor  $\sim 4.3$ .

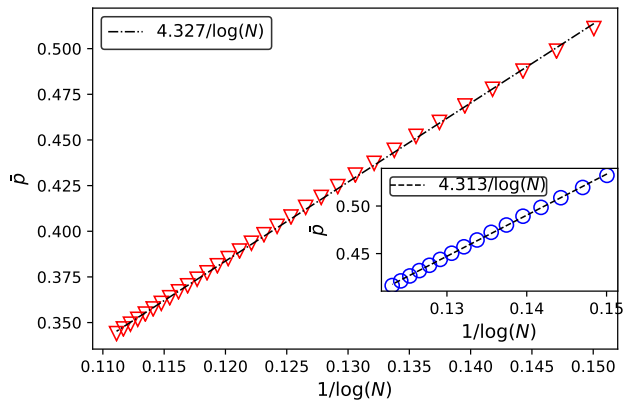


FIG. 4: Probability peak as a function of  $N$  for the nonlinear and linear algorithm (inset)

The Fig.5 shows the peak recurrence times,  $T$ , and  $T'$ . As expected, in the linear model, we recover  $T = O(\sqrt{N \log N})$ . The nonlinear case, instead, shows a significant advantage respect to the linear case, with a peak recurrence times  $T' \sim N^{1/4} \log^{3/4} N$ , which yields an overall complexity of  $O(N^{1/4} \log^{7/4} N)$ .

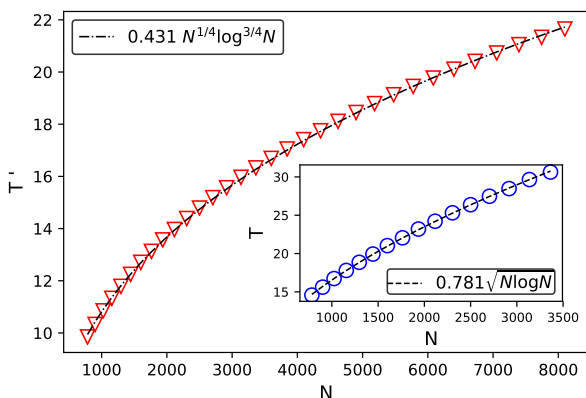


FIG. 5: Peak recurrence times in the nonlinear and the linear algorithm (inset).

#### IV. SCALE ANALYSIS

Although an exact analytical description is prohibitive, in this section we will provide some elements of analysis

that will convince the reader of the robustness of the numerical results obtained in the previous section. Let's start from the eigenvalues of Eq. 21, and rescale them using Eq. 23:

$$\lambda_{\pm} = \frac{1}{2}g\delta \pm \frac{1}{2}\sqrt{(g\delta)^2 + 4E^2(1 + cg\delta)^2} \quad (27)$$

Fixing  $g = \log N/\pi$  and  $c = \sqrt{\frac{N \log N}{64\pi}}$ , as in our numerical simulation, we can clearly distinguish two different behaviours for the probability  $|\alpha(t)|^2$ :

- A strictly linear regime, when  $\delta(t) = 0$ , which evolves periodically with a period

$$T_0 \sim 1/\Delta\lambda \sim \frac{1}{E} \sim \sqrt{N \log N} \quad (28)$$

- A nonlinear regime, when  $\delta(t)$  is maximum (and  $O(1/\log N)$ ). In this case, we have  $(1 + cg\delta(t)) \sim cg\delta(t) \sim \sqrt{N \log N}$  and the period is constant:

$$T_1 \sim 1/\Delta\lambda \sim 1. \quad (29)$$

Here, our aim will be to characterise how the system goes from the first regime to the second and under which conditions. Without a lack of generality, and because we are solely interested in the peak behaviour, we will focus on the first half period of the system dynamics. We propose the following ansatz:

$$|a(t)|^2 = \frac{A\pi}{\log N} \sin^2 \left( \frac{C_0 t}{T_0} + C_1 |a(t)|^2 \frac{t}{T_1} \right) \quad (30)$$

where  $A$ ,  $C_0$  and  $C_1$  are three real constants.

Let us try to justify this choice. First we can notice that the above self-consistent equation recovers both behaviours for the probability  $|\alpha(t)|^2$ : indeed, when  $|a(t=0)|^2 = 0$ , we get the Eq. (14), by choosing  $C_0 = 1$  and  $A = 1$ , and when  $|a|^2$  increases, the argument in the sinus increases as well, speeding-up the dynamics, as observed on Fig. 3. As  $T_1 \ll T_0$  and for large values of  $N$ , there exists a critical time  $t_s$  at which the Eq. (30) coincides with  $|a(t)|^2 = \frac{A\pi}{\log N} \sin^2 \left( C_1 |a(t)|^2 \frac{t}{T_1} \right)$ .

We may argue that the way  $t_s$  scales with  $N$ , may be the same one for the peak recurrence times. Numerical simulations shows that this is approximately true: in fact, in Fig. 6, the first probability peak is fitted, by several solutions of the Eq. (30), for several values of  $c$ . Along the first half period, the ansatz works surprisingly well.

Moreover, if we compute the characteristic time at which the system transits from the first behavior with period  $T_0$  to the second one with period  $T_1$ , we derive exactly the same scaling laws as  $T$  and  $T'$ . Say  $t_s$  is such a characteristic time, then at  $t_s$ , we have  $|a(t_s)|^2 t_s / T_1 \sim t_s / T_0$  and it follows:

$$\frac{1}{\log N} \sin^2(t_s/T_0) \sim T_1/T_0 \quad (31)$$

## VI. ACKNOWLEDGEMENTS

The authors acknowledge inspiring conversations with Thomas Wong. This work has been funded by the P epini ere d'Excellence 2018, AMIDEX fondation, project DiTiQuS and the ID 60609 grant from the John Templeton Foundation, as part of the ‘‘The Quantum Information Structure of Spacetime (QISS)’’ Project.

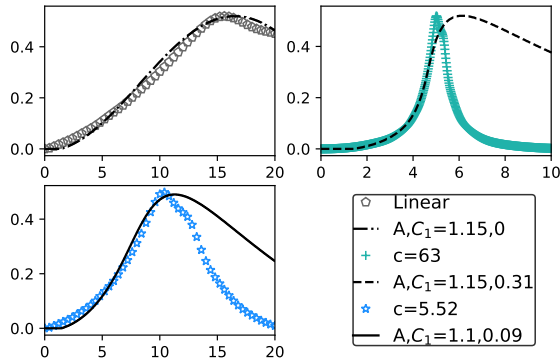


FIG. 6:  $N = 900$  - Probability over  $|\Gamma\rangle$  for different values of  $c$  and numerical resolution of eq. (30).

In conclusion, by keeping only the first term in the development of  $\arcsin x$  :

$$t_s \sim \sqrt{T_1 T_0 \log N} \quad (32)$$

and using Eqs. (28) and (29), we get

$$t_s \sim N^{1/4} \log^{3/4} N, \quad (33)$$

which confirms the numerical results we had in Sec. III for the probability peak time in the nonlinear algorithm.

## V. DISCUSSION

We proved numerically and analytically that nonlinear terms, embedded in the coined Quantum Walks lead to a strong computational advantage for spatial search algorithms, over the infinite square grid. The numerical simulations show that the walker finds the marked vertex in  $O(N^{1/4} \log^{3/4} N)$  steps with probability  $O(1/\log N)$ , for an overall complexity of  $O(N^{1/4} \log^{7/4} N)$ . These results are consistent with those ones proved by Wong and Meyer in [22] in the context of the nonlinear Schr odinger equation on the Hypercube. Our work presents numerous advantages respect the previous ones: (i) quantum walks are easily implementable in our labs by several physical systems; (ii) graphs having sets of vertices of constant size, are more natural and pave the way to a 3-dimensional generalisation; (iii) replacing the Grover oracle step by surface defects seems way more practical in terms of experimental realizations, whatever the substrate, possibly even in a biological setting. At a more abstract level, this suggests using QW to search, not just for ‘good’ configurations within a space, but rather for topological properties of the configuration space itself.

- 
- [1] Daniel S. Abrams and Seth Lloyd. Nonlinear quantum mechanics implies polynomial-time solution for  $\text{np-complete}$  and  $\text{pproblems}$ . *Physical Review Letters*, 81(18):3992–3995, Nov 1998.
- [2] Andrea Alberti and Sandro Wimberger. Quantum walk of a bose-einstein condensate in the brillouin zone. *Physical Review A*, 96(2):023620, 2017.
- [3] Andris Ambainis. Quantum walk algorithm for element distinctness. *SIAM Journal on Computing*, 37(1):210–239, 2007.
- [4] Pablo Arrighi, Giuseppe Di Molfetta, Iván Márquez-Martín, and Armando Pérez. Dirac equation as a quantum walk over the honeycomb and triangular lattices. *Physical Review A*, 97(6):062111, 2018.
- [5] Andrew M Childs. Universal computation by quantum walk. *Physical review letters*, 102(18):180501, 2009.
- [6] Andrew M Childs, Richard Cleve, Enrico Deotto, Edward Farhi, Sam Gutmann, and Daniel A Spielman. Exponential algorithmic speedup by a quantum walk. In *Proceedings of the thirty-fifth annual ACM symposium on Theory of computing*, pages 59–68, 2003.
- [7] Andrew M. Childs and Yimin Ge. Spatial search by continuous-time quantum walks on crystal lattices. *Physical Review A*, 89(5), May 2014.
- [8] Andrew M Childs and Jeffrey Goldstone. Spatial search by quantum walk. *Physical Review A*, 70(2):022314, 2004.
- [9] Giuseppe Di Molfetta and Pablo Arrighi. A quantum walk with both a continuous-time limit and a continuous-spacetime limit. *Quantum Information Processing*, 19(2):47, 2020.
- [10] Giuseppe Di Molfetta, Marc Brachet, and Fabrice Debbasch. Quantum walks as massless dirac fermions in curved space-time. *Physical Review A*, 88(4):042301, 2013.
- [11] Giuseppe Di Molfetta and Armando Pérez. Quantum walks as simulators of neutrino oscillations in a vacuum and matter. *New Journal of Physics*, 18(10):103038, 2016.
- [12] Lov K. Grover. A fast quantum mechanical algorithm for database search, 1996.
- [13] Mohamed Hatifi, Giuseppe Di Molfetta, Fabrice Debbasch, and Marc Brachet. Quantum walk hydrodynamics. *Scientific reports*, 9(1):1–7, 2019.
- [14] Mahdi Ebrahimi Kahou. *Spatial search via non-linear quantum walk*. PhD thesis, Citeseer, 2012.
- [15] Panayotis G Kevrekidis, Dimitri J Frantzeskakis, and Ricardo Carretero-González. *Emergent nonlinear phenomena in Bose-Einstein condensates: theory and experiment*, volume 45. Springer Science & Business Media, 2007.
- [16] Michael Maniaghala and Giuseppe Di Molfetta. Continuous time limit of the dtqw in  $2d+1$  and plasticity. *arXiv preprint arXiv:2007.01425*, 2020.
- [17] Giuseppe Di Molfetta, Fabrice Debbasch, and Marc Brachet. Nonlinear optical galton board: thermalization and continuous limit, 2015.
- [18] C. Navarrete-Benlloch, A. Pérez, and Eugenio Roldán. Nonlinear optical galton board. *Physical Review A*, 75(6), Jun 2007.
- [19] Mathieu Roget, Stéphane Guillet, Pablo Arrighi, and Giuseppe Di Molfetta. Grover search as a naturally occurring phenomenon. *Physical Review Letters*, 124(18):180501, 2020.
- [20] Yutaka Shikano, Tatsuki Wada, and Junsei Horikawa. Discrete-time quantum walk with feed-forward quantum coin. *Scientific reports*, 4:4427, 2014.
- [21] Salvador Elías Venegas-Andraca. Quantum walks: a comprehensive review. *Quantum Information Processing*, 11(5):1015–1106, 2012.
- [22] Thomas G. Wong. Nonlinear quantum search, 2015.